

Nonlinear transport properties of quantum dots

W. Pfaff¹, D. Weinmann^{1,2}, W. Häusler², B. Kramer², U. Weiss¹

¹ II. Institut für Theoretische Physik, Universität Stuttgart, Pfaffenwaldring 57, D-70550 Stuttgart, Germany

² I. Institut für Theoretische Physik, Universität Hamburg, Jungiusstrasse 9, D-20355 Hamburg, Germany

Received: 22 April 1994 / Revised version: 27 June 1994

Abstract. The influence of excited levels on nonlinear transport properties of a quantum dot weakly coupled to leads is studied using a master-equation approach. A charging model for the dot is compared with a quantum mechanical model for interacting electrons. The current-voltage curve shows Coulomb blockade and additional finestructure that is related to the excited states of the correlated electrons. Unequal coupling to the leads causes asymmetric conductance peaks. Negative differential conductances are predicted due to the existence of excited states with different spins.

PACS: 72.20.Ht; 73.20.Dx; 73.20.Mf; 73.40.Gk

I. Introduction

Periodic oscillations of the conductance through quantum dots that are weakly coupled to leads [1] are well established consequences of the charging energy of single electrons entering or leaving the dot at sufficiently low temperatures. They are observed in linear transport as a function of the carrier density. At bias voltages larger than the differences between discrete excitation energies within the dot, a characteristic splitting of the conductance peaks is observed [2, 3]. We will demonstrate unambiguously below that this is related to transport involving the excited states of n correlated electrons and that the shape of the peaks depends on the coupling between the quantum dot and the leads. Furthermore, it is shown that negative differential conductances can occur due to a ‘spin blockade’ [4] which is a consequence of the existence of excited states with different spins. Recently, negative differential conductances have also been found in the transport through a two-dimensional dot with parabolic confinement in the fractional quantum Hall effect (FQHE) regime without spin [5], where the origin of the effect are excited states for which the coupling to the leads is weaker than for the ground state.

II. Model

As a model for a quantum dot being weakly coupled to leads and capacitively influenced by the voltage applied to the gate electrode as schematically shown in Fig. 1, we consider the double barrier Hamiltonian

$$H = H_L + H_R + H_D + H_L^T + H_R^T + H^{in}, \quad (1)$$

where

$$H_{L/R} = \sum_k \varepsilon_k^{L/R} c_{L/R,k}^+ c_{L/R,k}$$

describes free electrons in the left/right lead and

$$H_D = \sum_l (\varepsilon_l - e\Phi) c_l^+ c_l + \sum_{l_1, l_2, l_3, l_4} V_{l_1 l_2 l_3 l_4} c_{l_1}^+ c_{l_2}^+ c_{l_3} c_{l_4}$$

the interacting electrons within the dot. The energies of the noninteracting electrons are ε_l and $V_{l_1 l_2 l_3 l_4}$ the matrix-elements of the Coulomb-interaction. The potential change in the dot Φ is due to the external voltages applied to the leads and the gate. In the experiment Φ is controlled by the voltage V_G that can be thought of being connected to the dot via a perfectly insulating ca-

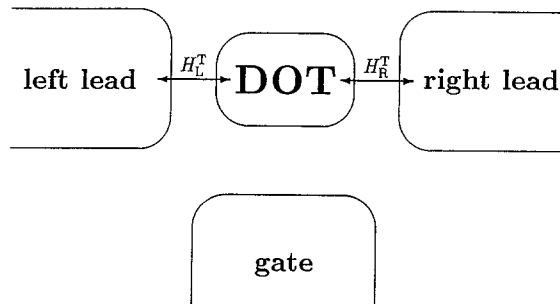


Fig. 1. Schematic picture of the quantum dot, the left/right and the gate electrode. The tunneling barriers $H_{L/R}^T$ are assumed to behave as (weakly transmissive) capacitors

pacitor. The variation of V_G serves to change the electron density in the well.

The barriers are represented by the tunneling Hamiltonians

$$H_{L/R}^T = \sum_{k,l} (T_{k,l}^{L/R} c_{L/R,k}^\dagger c_l + \text{h.c.}),$$

where $T_{k,l}^{L/R}$ are the transmission probability amplitudes which we assume to be independent of l . The inelastic term H^{in} allows for transitions between the dot levels without changing the electron number. A phononic heat bath and a Fröhlich type coupling (coupling constant \sqrt{g}) would be a microscopic model leading to such a term. We assume that the phase coherence between the eigenstates of $H - H^{\text{in}}$ is destroyed on a time scale τ_ϕ , which is much larger than the time an electron needs to travel from one barrier to the other. Thus, the motion of the electrons inside the dot is sufficiently coherent to guarantee the existence of quasi-discrete levels. We assume also that the leads are in thermal equilibrium described by the Fermi-Dirac-distributions

$$f_{L/R}(\varepsilon) = (\exp[\beta(\varepsilon - \mu_{L/R})] + 1)^{-1}.$$

The chemical potential in the left/right lead is $\mu_{L/R}$ and $\beta = 1/k_B T$ the inverse temperature. We assume the tunneling rates through the barriers

$$t^{L/R} = \frac{2\pi}{\hbar} \sum_k |T_{k,l}^{L/R}|^2 \delta(\varepsilon_k^{L/R} - E)$$

to be independent on energy E . If they are small compared to the phase breaking rate τ_ϕ^{-1} , the time-evolution of the occupation probabilities of the many-electron states in the dot can be calculated using a master-equation method which is described in the next section.

III. Method

In contrast to [6, 7], where changes in the occupation probabilities for one-electron levels were considered, we take into account the populations P_i of all possible Fock states $|i\rangle$ of H_D . Transitions between the latter occur when an electron tunnels through a barrier. Our method allows to determine the stationary non-equilibrium state without further restrictions. Deviations from equilibrium linear in the applied voltage have been mentioned in [8]. In addition the exact many-electron states of the dot including spin can be taken into account without being restricted to the conventional charging model. A similar method was applied in the FQHE regime without spin [5].

A. Transition rates due to tunneling

Due to the smallness of H^T , simultaneous transitions of two or more electrons [9] which are processes of higher order in H^T are suppressed. Further selection rules

will be specified below. Each of the states $|i\rangle$ is associated with a certain electron number n_i and with an energy eigenvalue E_i . The transition rates between states $|i\rangle$ and $|j\rangle$ with $n_i = n_j + 1$ are given by $\Gamma_{j,i}^{L/R,-}$ and $\Gamma_{i,j}^{L/R,+}$, depending on whether an electron is leaving or entering the dot through the left/right barrier, respectively. A straightforward perturbation theory calculation in lowest order in H^T yields

$$\Gamma_{j,i}^{L/R,-} = t^{L/R} [1 - f_{L/R}(E)]$$

$$\Gamma_{i,j}^{L/R,+} = t^{L/R} f_{L/R}(E)$$

and the electron provides the energy difference $E = E_i - E_j$.

B. Inelastic transitions due to electron-phonon processes

Assuming a bosonic heat bath being weakly coupled to the electrons, the transition rate between $|i\rangle$ and $|j\rangle$ ($n_i = n_j$) induced by H^{in} is given by

$$\Gamma_{j,i}^{\text{in}} = r [n_B(|E|) + \Theta(E)],$$

where $r = g \rho_{\text{ph}}$. This is the lowest order result quadratic in the electron-heat bath coupling strength \sqrt{g} . ρ_{ph} is the boson density of states,

$$n_B(E) = (\exp[\beta E] - 1)^{-1}$$

the Bose-Einstein-distribution and $\Theta(x)$ the step function.

C. Master equation and DC-current

The full matrix of transition rates is

$$\Gamma = \Gamma^{L,+} + \Gamma^{R,+} + \Gamma^{L,-} + \Gamma^{R,-} + \Gamma^{\text{in}}.$$

The master equation for the time evolution of the occupation probabilities P_i is

$$\frac{d}{dt} P_i = \sum_{j(j \neq i)} (\Gamma_{i,j} P_j - \Gamma_{j,i} P_i), \quad \sum_i P_i = 1. \quad (2)$$

From the stationary solution ($d\bar{P}_i/dt = 0$) of (2) one determines the dc-current

$$I \equiv I^{L/R} = (-/+) e \sum_{i,j(j \neq i)} \bar{P}_j (\Gamma_{i,j}^{L/R,-} - \Gamma_{i,j}^{L/R,+}).$$

It equals the number of electrons that pass the left/right barrier per unit of time.

IV. Results

A. Charging Model

As a tutorial example we consider the phenomenological charging model [6–8] for N single-electron levels, where

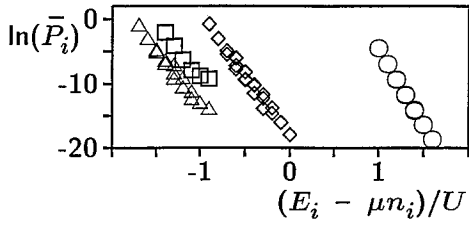


Fig. 2. Stationary occupation probabilities \bar{P}_i for a dot containing $N=6$ one-electron levels. Electron numbers are $n_i=1$ (\square), $n_i=2$ (\triangle), $n_i=3$ (\diamond) and $n_i=4$ (\circ). Some of the data points for $n_i=4$ with $\ln(\bar{P}_i) < 20$ are not shown in this figure. $t^L=t^R$, $\mu_L=1.5U$, $\mu_R=-0.3U$, $\mu=(\mu_L+\mu_R)/2$ and $\Phi=0$. Energies of the one-electron levels are $\varepsilon_1=0.1U$, $\varepsilon_2=0.2U$, $\varepsilon_3=0.3U$, $\varepsilon_4=0.4U$, $\varepsilon_5=0.5U$ and $\varepsilon_6=0.6U$. Inverse temperature is $\beta=25/U$ and the relaxation rate $r=100\bar{t}$. $\bar{t}=t^L t^R/(t^L+t^R)$ is the total transmission rate

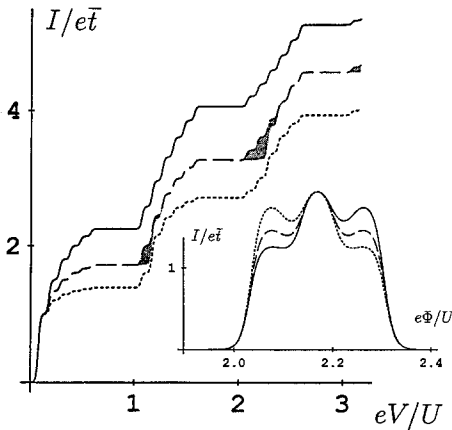


Fig. 3. Current-voltage characteristic of a dot represented by $N=6$ one-electron levels. Model parameters are as in Fig. 2. Inverse temperature is $\beta=100/U$, $\mu_R=0$. Inset: Current versus V_G for $\mu_L=0.26U$ and $\mu_R=0$. $V=0.26U/e$ is between the double and the triple of the bare level-spacing such that the conductance peaks are modulated as explained in the text. Dashed lines: results for $r=0$ and equal barriers, dotted and solid lines: $t^R/t^L=0.5$ and 2 , respectively. Shaded regions: suppressions of steps induced by relaxation $r/\bar{t}=100$ at $t^L=t^R$

$$V_{l_1 l_2 l_3 l_4} = (U/2) \delta_{l_1, l_4} \delta_{l_2, l_3}.$$

The stationary solution of (2) was obtained by solving numerically the system of 2^N linear equations.

1. Stationary occupation probabilities. At zero bias voltage the occupation probabilities of the n -electron states are given by a Gibbs distribution

$$P_i^G = (\exp[-\beta(E_i - \mu n_i)]) / \mathcal{Z}$$

with the chemical potential $\mu = \mu_L = \mu_R$. They solve the rate equation (2) for all r . \mathcal{Z} is the grand canonical partition function. For temperatures lower and voltages higher than the level-spacings, \bar{P}_i deviate from equilibrium. For $r \gg t^{L/R}$ (fast equilibration via bosons) \bar{P}_i/\bar{P}_j can be satisfactorily approximated by P_i^G/P_j^G for $n_i=n_j$. This can be seen in Fig. 2 where $\ln \bar{P}_i$ for a given n_i lie on straight lines with slope $-\beta$. This confirms the assumptions of a Gibbs distribution among states with given

electron number in [7, 8]. When $n_i \neq n_j$, \bar{P}_i/\bar{P}_j can be far from equilibrium. It is impossible to scale all of the points onto one common curve by defining an effective chemical potential for the dot [10].

2. Current-voltage-characteristics. The current-voltage characteristics (Fig. 3) for temperatures lower than the level-spacing shows finestructure in the Coulomb staircase consistent with recent experiments [2] and earlier theoretical predictions using a different approach [6]. To avoid artifacts arising from the finite number of one-electron levels we do not plot the part arising from states with $n > 3$ and discuss only the realistic case $n < N$. Intradot relaxation ($\sim r$) suppresses the lowest of the finestructure steps because the electron that contributes to the current at the n -th Coulomb step has to enter the n -th or a higher one-electron level. For $r \gg t^{L/R}$ the $n-1$ other electrons occupy with high probability all of the lower one-electron levels. Asymmetric coupling to the leads changes the height of the steps in the $I-V$ curve. This can be explained for the n -th Coulomb step as follows. If $t^L > t^R$ ($\mu_L > \mu_R$) the stationary occupation probabilities favor the n -electron levels, while for $t^L < t^R$ the $(n-1)$ -electron states are preferred. Since there are more n -electron levels than $(n-1)$ -electron levels, the probability for an electron to escape is reduced in the former case as compared to the probability for an electron to enter in the latter case. These processes limit the current. They lead to a reduction and an enhancement of the current in the first and second case, respectively.

3. Splitting of conductance peaks. For fixed V , the conductance shows peaks when V_G is varied. The linear response limit of our method is in agreement with [11]. For finite bias voltage, $eV = \mu_L - \mu_R$, larger than the level spacing, transitions involving excited states can occur. The number of levels that contribute to the current varies when V_G is changed. This leads to the splitting of the conductance peaks observed experimentally and explained qualitatively in [2, 12]. From the quantitative treatment of the charging model using (2) for $T=0$, i.e. only constant nonvanishing or vanishing $F_{i,j}$'s, we obtain that the number of transitions contributing to the current varies with V_G as $0-6-4-12-4-6-0$ in the specific example shown for finite temperature in Fig. 3, inset. Taking into account the stationary \bar{P}_i 's the sequence of current values is $0-3/2-4/3-2-4/3-3/2-0$. If the difference $E_0(n) - E_0(n-1)$ between the energies of the many electron ground states lies outside the interval $[\mu_R, \mu_L]$ the transport via other energetically allowed transitions is Coulombically blocked. While the relaxation rates have almost no influence on the conductance, asymmetric coupling to the leads changes the shape of the peaks considerably. We propose to explain the slight asymmetry observed in the experiment [2, 13] by the asymmetry of the barriers. The asymmetry in the finestructure of the observed conductance peaks will be reversed if the sign of the bias voltage is changed. Such asymmetric conductance properties can be used to construct a mesoscopic rectifier. Similar effects were inferred earlier from the high frequency properties of mesoscopic systems containing asymmetric disorder [14].

B. Correlated electron model

However, the charging model is a severe simplification for interacting electrons, especially for systems with reduced dimensionality. Therefore, we consider as a second example $n \leq 4$ interacting electrons in a quasi one-dimensional (1D) square well of length L including the spin degree of freedom [15–17]. Therefore, the dot Hamiltonian now reads

$$H_D = \sum_{l,\sigma} (\varepsilon_l - e\Phi) c_{l,\sigma}^\dagger c_{l,\sigma} + \sum_{\substack{l_1, l_2, l_3, l_4 \\ \sigma_1, \sigma_2}} V_{l_1 l_2 l_3 l_4} c_{l_1, \sigma_1}^\dagger c_{l_2, \sigma_2}^\dagger c_{l_3, \sigma_2} c_{l_4, \sigma_1}.$$

1. Spectrum. We calculated numerically the exact eigenvalues E_ν and the corresponding n -electron states $|y\rangle$ for this correlated electron model. The interaction potential

$$V(x, x') \propto ((x - x')^2 + \lambda^2)^{-1/2}$$

was used, where $\lambda (\ll L)$ is a low distance cutoff due to a transversal spread of the electronic wave function. Since the interaction is spin independent, the n -electron spin S is a good quantum number. The properties of the correlated states and the energy spectrum are discussed in detail in [15, 16]. For not too large electron densities tendency towards Wigner crystallization is found [17]. In this regime, the excitation spectrum consists of well separated multiplets, each containing 2^n states. The energetic differences between adjacent multiplets decrease algebraically with electron density. They correspond to excitations of (almost) harmonic motions of the separated electrons repelling each other by Coulomb forces. These are phonon like excitations. Quantum corrections split the 2^n -fold degenerate levels at increasing electron densities. They can be traced back [15] to processes where electrons exchange their positions by tunneling through a Coulomb potential barrier. The corresponding tunneling integral t_n for n electrons sets the energy scale for this splitting. The considerably smaller intra-multiplet energy differences decrease exponentially with the electron density. The wave functions of individual levels within a given multiplet differ in symmetry and S . For $n \leq 4$, the excitation energies in the lowest multiplet can be calculated analytically [18] and depend only on one tunneling integral t_n (Table 1). In summary, two different energy scales characterize the n -electron excitations. We will now demonstrate that they can be distinguished in principle by a nonlinear transport experiment.

2. Spin selection rules. As an additional selection rule, we take into account that each added or removed electron can change the total spin S of the n electrons in the dot only by $\pm 1/2$ with probabilities $(S+1)/(2S+1)$ and $S/(2S+1)$, respectively. The values of these spin factors are found from a sum over the corresponding Clebsch-Gordan coefficients and enter the transition rates as prefactors. We emphasize here again that this

Table 1. Spin and energies of low lying excitations of the correlated electron model at sufficiently large electron distances $r_s \equiv L/(n-1) \gg a_B$. The tunneling integrals t_n decrease exponentially with r_s

n	S	$E_i - E_0(n)$
2	0	0
2	1	$2t_2$
3	1/2	0
3	1/2	$2t_3$
3	3/2	$3t_3$
4	0	0
4	1	$(1 - \sqrt{2} + \sqrt{3})t_4$
4	1	$(1 + \sqrt{3})t_4$
4	0	$(2\sqrt{3})t_4$
4	1	$(1 + \sqrt{2} + \sqrt{3})t_4$
4	2	$(3 + \sqrt{3})t_4$

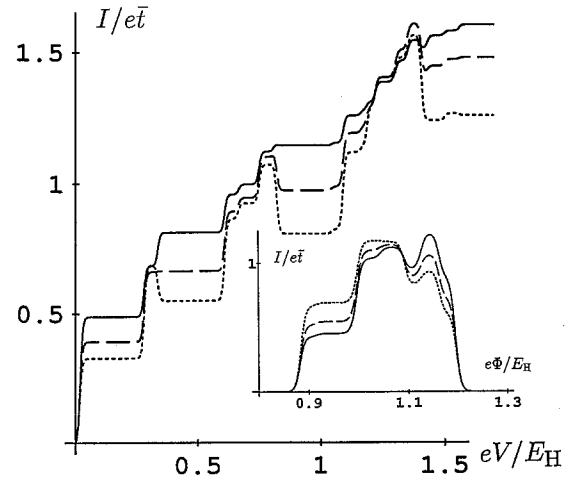


Fig. 4. Current-voltage characteristic ($\mu_R = 0, \Phi = 0$) and the splitting of the fourth conductance peak at $\mu_L = 0.3 E_H$ and $\mu_R = 0$ (inset) of a dot described by the correlated electron model for $\beta = 200/E_H$ ($E_H \equiv e^2/a_B$ Hartree-energy) and $r = \bar{r}$. Tunneling integrals are $t_2 = 0.03 E_H$, $t_3 = 0.07 E_H$ and $t_4 = 0.09 E_H$, numerically determined ground state energies $E_0(1) = 0.023 E_H$, $E_0(2) = 0.30 E_H$, $E_0(3) = 0.97 E_H$, $E_0(4) = 2.15 E_H$. Dashed, dotted and solid lines correspond to $t^R/t^L = 1, 0.5$ and 2 , respectively

can be done only by considering all possible Fock states in the rate equation (2).

3. Current-voltage characteristics. Occupation probabilities are similar as for the charging model but modified by spin effects. Current-voltage characteristics and conductivity peaks calculated by using the excitation energies given in Table 1 are shown in Fig. 4. First of all, we observe that the lengths of the steps in the Coulomb staircase and accordingly the distances of the conductivity peaks are no longer equal since the exact n -electron ground state energy is not proportional to $n(n-1)$ as in the charging model for small ε_i 's. The deviation from the classical behavior is related to the inhomogeneity of the quantum mechanical charge density of the ground state [15]. Second, the heights of the finestructure steps are more random as compared to those in Fig. 3 due to the non-regular sequence of total spins (cf. Table 1)

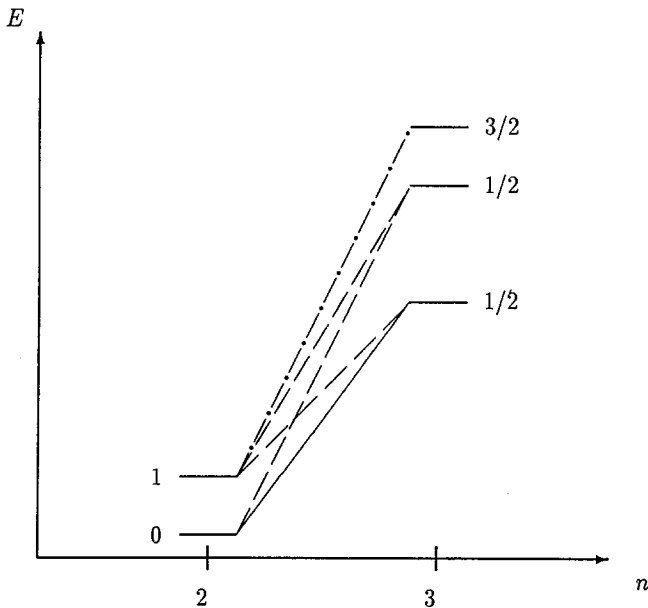


Fig. 5. Dot states for $n_i=2$ and $n_i=3$. The lines represent transitions that are allowed by the selection rules. In linear transport, only the ground state to ground state transition (solid line) determines the transport. At finite transport voltage additionally transitions between excited states come into play. Since the transition to the highest state (dotted) is a ‘dead end’, the current is reduced when the voltage is raised to a value that allows the system to go into the highest state

and the spin selection rules. In certain cases finestructure steps in the $I-V$ characteristic may even be completely suppressed.

4. Spin blockade effect. Strikingly, regions of negative differential conductance occur (Fig. 4). They are related to the reduced possibility for the states of maximal spin $S=n/2$ to decay into states of lower electron number [4]. In Figure 5, the states involved in transitions between $n=2$ and $n=3$ electron numbers are shown together with the transitions allowed by the spin selection rules. The 3-electron state of maximal spin $S=3/2$ has only one possibility to reduce its electron number. Therefore, the lifetime of this state is significantly larger than for the other states. If the applied voltage V allows for the occupation of this state, it attracts a considerable amount of the stationary occupation probability. The reduced occupation of the other states leads to a reduced current. The state with polarized spin appears only once within each multiplet for given electron number. Therefore only one finestructure step with negative differential conductance can occur within each Coulomb step. The peak in the $I-V$ curve can become less pronounced if $t^L < t^R$, because then the dot is empty and the $(n-1) \rightarrow n$ transitions determine the current. The spin selection rules reduce the probability for $n \rightarrow (n-1)$ transitions (especially important for $t^L > t^R$) and the negative differential conductance becomes more pronounced (Fig. 4). Such a behavior can in fact be seen in the experimental data [2, 19] but certainly needs much more elaborate further investigations. These negative differential con-

ductances can in principle be used to construct a mesoscopic oscillator.

V. Summary

In summary, we have investigated nonlinear transport through a double barrier taking into account Coulomb interactions, spin and non-equilibrium effects. For two model Hamiltonians occupation probabilities, current-voltage characteristics and conductances versus gate-voltage at finite bias voltage have been calculated using a master equation approach.

Thermally induced intra-dot relaxation processes lead to a suppression of the n lowest finestructure steps in the n -th Coulomb step of the $I-V$ curve. At finite bias voltages, the intra-dot relaxation results in thermal equilibrium only among the states with equal dot electron number. We have demonstrated explicitly that the stationary non-equilibrium populations cannot be described by a Gibbs distribution. Asymmetric barriers cause pronounced asymmetries in the conductance peaks versus gate-voltage. We predict the reversal of the asymmetry when the bias voltage is reversed. Taking into account the quantum mechanics of Coulombically interacting electrons including their spins leads to striking modifications of the transport as compared to the charging model. First of all, the Coulomb blockade intervals in the $I-V$ characteristic and the distances between the conductance peaks are no longer constant. Because of spin selection rules for the correlated electron system, the heights of the single steps in the finestructure of the Coulomb staircase look random. Furthermore, regions of negative differential conductance occur because for each electron number the one state of maximum spin has a reduced transition probability into states with lower electron number. This general feature of a ‘spin blockade’ is not restricted to the quasi-1D model considered here but should also apply to 2D dots used in experiments containing few electrons. All of the theoretically predicted features described above are qualitatively consistent with experiment [2]. Further experiments, in particular using ‘slim quantum dots’, are however necessary in order to clarify the quantitative aspects.

Preliminary results taking into account a magnetic field in transport direction show that the occurrence of negative differential conductance is suppressed when the Zeeman splitting becomes larger than the excitation energies of the dot states. To clarify these questions and to be able to make quantitative comparisons with existing experimental data, generalization of the above correlated electron model to 2D is necessary.

For valuable discussions we thank R. Haug and J. Weis. We thank the PTB Braunschweig, where a part of this work was done, for the kind hospitality. This work was supported in part by the Deutsche Forschungsgemeinschaft via grants We 1124/2-2, We 1124/4-1 and AP 47/1-1 and by the European Community within the Science program, grant SCC*-CT90-0020.

References

1. Meirav, U., Kastner, M.A., Wind, S.J.: Phys. Rev. Lett. **65**, 771 (1990); Kastner, M.A.: Rev. Mod. Phys. **64**, 849 (1992)
2. Johnson, A.T., Kouwenhoven, L.P., Jong de, W., Vaart, N.C. van der, Harmans, C.J.P.M., Foxon, C.T.: Phys. Rev. Lett. **69**, 1592 (1992)
3. Weis, J., Haug, R.J., Klitzing, K.v., Ploog, K., Phys. Rev. **B46**, 12837 (1992)
4. Weinmann, D., Häusler, W., Pfaff, W., Kramer, B., Weiss, U.: Europhys. Lett. **26**, 467 (1994)
5. Kinaret, J.M. et al.: Phys. Rev. **B46**, 4681 (1992)
6. Averin, D.V., Korotkov, A.N.: J. Low Temp. Phys. **80**, 173 (1990)
7. Averin, D.V., Korotkov, A.N., Likharev, K.K.: Phys. Rev. **B44**, 6199 (1991)
8. Beenakker, C.W.J.: Phys. Rev. **B44**, 1646 (1991)
9. Averin, D.V., Odintsov, A.A.: Phys. Lett. **A140**, 251 (1989); Averin, D.V., Nazarov, Yu.V.: In: Single charge tunneling. Grabert, H., Devoret, M.H. (eds.) New York: Plenum Press 1991
10. The linear correction to the Gibbs distribution calculated in [8] vanishes for the case shown in Fig. 2
11. Meir, Y., Wingreen, N.S., Lee, P.A.: Phys. Rev. Lett. **66**, 3048 (1991)
12. Foxman, E.B. et al.: Phys. Rev. **B47**, 10020 (1993)
13. Vaart van der, N.C., Johnson, A.T., Kouwenhoven, L.P., Maas, D.J., Jong de, W., de Ruyter van Stevenick, M.P., Enden, van der A., Harmans, C.J.P.M.: Physica **B189**, 99 (1993)
14. Fal'ko, V.I.: Europhys. Lett. **8**, 785 (1989)
15. Häusler, W., Kramer, B., Mašek, J.: Z. Phys. **B85**, 435 (1991); Häusler, W., Kramer, B., Phys. Rev. **B47**, 16353 (1993)
16. Brandes, T., Häusler, W., Jauregui, K., Kramer, B., Weinmann, D.: Physica **B189**, 16 (1993)
17. Jauregui, K., Häusler, W., Kramer, B.: Europhys. Lett. **24**, 581 (1993)
18. Häusler, W.: (Preprint 1994)
19. Weis, J., Haug, R.J., Klitzing v., K., Ploog, K.: Phys. Rev. Lett. **71**, 4019 (1993)